# Benzoxazinoid Metabolites Regulate Innate Immunity against Aphids and Fungi in Maize[1][W][OA]

**Shakoor Ahmad, Nathalie Veyrat, Ruth Gordon-Weeks, Yuhua Zhang, Janet Martin, Lesley Smart, Gaétan Glauser, Matthias Erb, Victor Flors, Monika Frey, and Jurriaan Ton***

Rothamsted Research, Centre for Sustainable Pest and Disease Management, Harpenden AL5 4JQ, United Kingdom (S.A., N.V., R.G.-W., Y.Z., J.M., L.S., J.T.); Laboratory for Fundamental and Applied Research in Chemical Ecology (N.V., G.G., M.E.) and Chemical Analytical Service of the Swiss Plant Science Web (G.G.), University of Neuchâtel, CH–2009 Neuchatel, Switzerland; Plant Physiology Section, Department of Experimental Sciences, University of Jaume I, 12071 Castellon, Spain (V.F.); Lehrsuhl für Genetik, Technische Universität München, 85 354 Freising, Germany (M.F.); Faculty of Science, Plant-Microbe Interactions, Institute of Environmental Biology, Utrecht University, 3508 TB Utrecht, The Netherlands (S.A.); and Department of Animal and Plant Sciences, University of Sheffield, Sheffield S102TN, United Kingdom (J.T.)

Benzoxazinoids (BXs), such as 2,4-dihydroxy-7-methoxy-2H-1,4-benzoxazin-3(4H)-one (DIMBOA), are secondary metabolites in grasses. The first step in BX biosynthesis converts indole-3-glycerol phosphate into indole. In maize (*Zea mays*), this reaction is catalyzed by either BENZOXAZINELESS1 (BX1) or INDOLE GLYCEROL PHOSPHATE LYASE (IGL). The *Bx1* gene is under developmental control and is mainly responsible for BX production, whereas the *Igl* gene is inducible by stress signals, such as wounding, herbivory, or jasmonates. To determine the role of BXs in defense against aphids and fungi, we compared basal resistance between *Bx1* wild-type and *bx1* mutant lines in the *igl* mutant background, thereby preventing BX production from IGL. Compared to *Bx1* wild-type plants, BX-deficient *bx1* mutant plants allowed better development of the cereal aphid *Rhopalosiphum padi*, and were affected in penetration resistance against the fungus *Setosphaeria turtica*. At stages preceding major tissue disruption, *R. padi* and *S. turtica* elicited increased accumulation of DIMBOA-glucoside, DIMBOA, and 2-hydroxy-4,7-dimethoxy-1,4-benzoxazin-3-one-glucoside (HDMBOA-glc), which was most pronounced in apoplastic leaf extracts. Treatment with the defense elicitor chitosan similarly enhanced apoplastic accumulation of DIMBOA and HDMBOA-glc, but repressed transcription of genes controlling BX biosynthesis downstream of BX1. This repression was also obtained after treatment with the BX precursor indole and DIMBOA, but not with HDMBOA-glc. Furthermore, BX-deficient *bx1* mutant lines deposited less chitosan-induced callose than *Bx1* wild-type lines, whereas apoplast infiltration with DIMBOA, but not HDMBOA-glc, mimicked chitosan-induced callose. Hence, DIMBOA functions as a defense regulatory signal in maize innate immunity, which acts in addition to its well-characterized activity as a biocidal defense metabolite.

Induced plant defense against pests and diseases encompasses a wide variety of mechanisms, ranging from deposition of callose-rich papillae to accumulation of biocidal defense metabolites. Defensive metabolites can be synthesized de novo in response to microbe or insect attack, such as phytoalexins, but can also be produced constitutively and stored as an inactive form in the plant cell. These so-called phytoanticipins can be activated by $\beta$-glucosidase activity during herbivory, which allows for a rapid release of biocidal aglycone metabolites (VanEtten et al., 1994; Morant et al., 2008). Well-characterized examples of phytoanticipins are glucosinolates (GSs), which can be hydrolyzed by endogenous $\beta$-thioglucoside glucohydrolases, called myrosinases. Although GSs have traditionally been associated with defense against herbivores, recent insights have revealed that they can also play a role in resistance against microbes. For instance, Bednarek et al. (2009) demonstrated in Arabidopsis (*Arabidopsis thaliana*) that early acting penetration resistance against powdery mildew requires biosynthesis of the indolic GS 4-methoxyindol-3-ylmethylglucosinolate (4MI3G) and subsequent hydrolysis by the atypical myrosinase PEN2. Furthermore, penetration resistance of Arabidopsis against *Phytophthora brassicae* depends on the sequential action of the same class of indolic GSs and the indolic phytoalexin camalexin (Schlaeppi et al., 2010; Schlaeppi and Mauch, 2010). Interestingly, Clay et al. (2009) reported that callose deposition after treatment with the flagellin epitope flg22 requires intact biosynthesis and breakdown of 4MI3G. This finding uncovered a novel signaling role by indolic GSs in Arabidopsis

[1] This work was supported by a Biotechnology and Biological Sciences Research Council Institute Career Path Fellowship (no. BB/E023959/1 to J.T.).

* Corresponding author; e-mail jurriaan.ton@bbsrc.ac.uk.

The author responsible for distribution of materials integral to the findings presented in this article in accordance with the policy described in the Instructions for Authors (www.plantphysiol.org) is: Jurriaan Ton (jurriaan.ton@rothamsted.ac.uk or j.ton@sheffield.ac.uk).

[W] The online version of this article contains Web-only data.

[OA] Open Access articles can be viewed online without a subscription.

www.plantphysiol.org/cgi/doi/10.1104/pp.111.180224

  

immunity, but also raises the question of how callose deposition is regulated in non-Brassicaceous plants, which do not produce GSs.

Benzoxazinoids (BXs) are widely distributed phytoanticipins among Poaceae. It is commonly assumed that BX-glucosides are hydrolyzed by plastid-targeted β-glucosidases upon tissue disruption, which results in the release of biocidal aglycone BXs (Morant et al., 2008). Since their discovery as plant secondary metabolites, many investigations have focused on their role in plant defense against herbivorous insects and pathogens (Niemeyer, 1988, 2009). Most of these studies revealed positive correlations between resistance and BX levels in cereal varieties or inbred populations, or biocidal activity when added to artificial growth medium (for review, see Niemeyer, 2009). In maize (*Zea mays*), defense elicitation by pathogenic fungi or treatment with the defense regulatory hormone jasmonic acid (JA) influences BX metabolism by promoting the conversion of 2,4-dihydroxy-7-methoxy-2H-1,4-benzoxazin-3(4H)-one-glucoside (DIMBOA-glc) into *N*-*O*-methylated 2-hydroxy-4,7-dimethoxy-1,4-benzoxazin-3-one-glucoside (HDMBOA-glc) (Oikawa et al., 2002, 2004). When supplied to artificial growth medium, HDMBOA-glc is more effective than DIMBOA-glc in reducing survival rates of the aphid *Metopolophium dirhodum* (Cambier et al., 2001).

The biosynthesis of BXs is mostly under developmental control and leads to accumulation of inactive BX-glucosides that are stored in the vacuole (Frey et al., 2009). In rye (*Secale cereale*) and wild barley (*Hordeum vulgare*), 2,4-dihydroxy-2H-1,4-benzoxazin-3(4H)-one (DIBOA) is the dominant BX, whereas the methoxy derivative DIMBOA is more prevalent in maize and wheat (*Triticum aestivum*; Niemeyer, 2009). The *BENZOXAZINELESS1* (*Bx1*) gene mediates the first dedicated step in the BX pathway and encodes a close homolog of the Trp synthetase α-subunit, which catalyzes the formation of indole from indole-3-glycerole phosphate (Frey et al., 1997; Melanson et al., 1997). This compound is subsequently oxidized by four cytochrome P450 monooxygenases, BX2 to BX5, into DIBOA (Frey et al., 1997), which can then be glucosidated by the glucosyltransferases BX8 and BX9 (von Rad et al., 2001). Elucidation of the final reactions toward DIMBOA-glc revealed that the cytosolic dioxygenase BX6 and methyltransferase BX7 mediate conversion of DIBOA-glc via 2,4,7-trihydroxy-1,4-benzoxazin-3(4H)-one-glucoside into DIMBOA-glc (Jonczyk et al., 2008). Upon tissue disruption, DIBOA-glc and DIMBOA-glc can be hydrolyzed by two plastid-targeted β-glucosidases, ZmGLU1 and ZmGLU2 (Cicek and Esen, 1999; Czjzek et al., 2001), which causes the release of biocidal DIBOA and DIMBOA aglycones. This mode of action is consistent with a role for BXs in resistance against chewing herbivores that cause major tissue damage. However, BXs have also been implicated in defense against aphids and pathogenic fungi that cause relatively little tissue damage (Niemeyer, 2009), which suggests an alternative mechanism of BX-dependent resistance.

Apart from BX1, the BX1 homolog INDOLE-3-GLYCEROL PHOSPHATE LYASE (IGL) can also convert indole-3-glycerole phosphate into free indole (Frey et al., 2000). The enzymatic properties of IGL are similar to BX1, but the transcriptional regulation of their corresponding genes is different. Like other *Bx* genes, *Bx1* is constitutively expressed during the early developmental stages of the plant, which correlates with endogenous BX levels. Plants carrying the mutant alleles of the *Bx1* gene produce only a fraction of the BXs that are found in *Bx1* wild-type plants (approximately 1.5%; Supplemental Figs. S1 and S2). Hence, the BX1 enzyme is accountable for the bulk of BX biosynthesis, whereas the functionally equivalent IGL enzyme appears to have a minor contribution in unstressed maize seedlings. Indeed, the *Igl* gene is expressed at much lower levels than *Bx1* during seedling development (Frey et al., 2000), explaining why it largely fails to complement BX production in seedlings of the *bx1* mutant. Unlike *Bx1*, the expression of *Igl* correlates tightly with the emission of volatile indole: Defense-eliciting stimuli, such as herbivore feeding, wounding, the insect elicitor volicitin, and methyl jasmonate, all stimulate *Igl* expression and indole emission (Frey et al., 2000, 2004), suggesting transcriptional regulation by the JA pathway. It has been proposed that herbivore-induced indole emission contributes to attraction of natural enemies, such as parasitoid wasps. Nevertheless, using pharmacological treatments to inhibit indole production, D'Alessandro et al. (2006) reported no or even a repellent effect by indole on parasitoid behavior. Interestingly, the *bx1* single mutant can accumulate up to up to 20% of wild-type BX levels after caterpillar infestation (N. Veyrat, personal communication). Furthermore, treatment of the *bx1* single mutant with indole can rescue DIMBOA production (Frey et al., 1997; Melanson et al., 1997). Hence, IGL has the potential to complement the *bx1* mutation and contribute to in planta BX biosynthesis during expression of JA-dependent defense.

In this study, we have investigated the role of BXs in maize defense against plant attackers that do not cause major tissue disruption. We compared basal resistance against the bird cherry oat aphid, *Rhopalosiphum padi*, and the pathogenic fungus *Setosphaeria turtica* between wild-type and *bx1* mutant lines in the *igl* mutant background, thereby blocking BX production from stress-induced IGL. We demonstrate that *Bx1*-dependent BXs play a critical role in basal resistance against aphids and fungi, which manifests itself as increased deposition of BXs in the apoplast. Moreover, we provide evidence that extracellular DIMBOA regulates pathogen-associated molecular pattern (PAMP)-induced callose and *Bx* gene expression, thereby uncovering a novel regulatory function of this compound in cereal innate immunity against pests and diseases.

## RESULTS

### Selection of Single and Double Mutants in *lgl* and *Bx1*

The *Igl* gene is inducible by herbivory, tissue wounding, volicitin, and methyl jasmonate (Frey et al., 2000, 2004), suggesting transcriptional regulation by the JA response pathway. It is, therefore, plausible that plants with a dysfunctional *Bx1* gene can accumulate BX levels from the stress-inducible IGL enzyme. Consequently, the *bx1* single mutant is unsuitable to assess the contribution of BXs to resistance against JA-eliciting attackers, such as *R. padi* and *S. turtica* (Delp et al., 2009; Erb et al., 2009). We, therefore, created *Bx1* wild-type and *bx1* mutant plants in the genetic background of a dysfunctional *Igl* gene. To this end, a *Mutator* (*Mu*)-induced mutant in the *Igl* gene was crossed with the original *bx1bx1* mutant (Hamilton, 1964). Homozygous mutants in progenies from two independent crosses were selected and confirmed by HPLC analysis of BX leaf content, and gas chromatography analysis of wound-inducible indole emission (Supplemental Figs. S1 and S2). This selection resulted in three confirmed genotypes from each cross: the indole-producing *bx1* single mutant (*bx1 Igl*), the indole-deficient *igl* single mutant (*Bx1 igl*), and the BX- and indole-deficient double mutant (*bx1 igl*).

### *Bx1* Is Required for Basal Resistance against Aphids

To establish the role of BXs in basal resistance against aphids, we compared growth and survival rates of *R. padi* between *Bx1* wild-type lines (*Bx1 igl*) and *bx1* mutant lines (*bx1 igl* and *bx1 Igl*) from both crosses. After 7 d of feeding from the first leaf, aphids gained significantly less weight when placed on BX-producing *Bx1 igl* lines compared to BX-deficient *bx1 igl* and *bx1 Igl* lines (Fig. 1A). In addition, the percentage of aphid survival was less than 10% after feeding from the *Bx1* wild-type lines, whereas over 70% remained alive after feeding from the *bx1* mutant lines (Fig. 1B). These differences were similar in progenies from both crosses and indicate a major contribution from the *Bx1* gene to basal resistance against *R. padi*. Interestingly, aphids reared on the *bx1* single mutant from the second cross showed marginally lower levels of survival than the corresponding *bx1 igl* double mutant (Student's *t* test; $P = 0.048$), suggesting a relatively small contribution from the *Igl* gene.

### Aphid Infestation Stimulates Apoplastic BX Accumulation

To examine which BX compounds contribute to *Bx1*-dependent resistance against *R. padi*, we quantified BX profiles after 2 d of feeding from BX-producing wild-type plants. Analysis of whole-leaf extracts by HPLC-diode array detection (DAD) identified three major BX compounds: DIMBOA-glc, DIMBOA, and HDMBOA-glc (Fig. 2A), which were confirmed by ultra-high-pressure liquid chromatography coupled to quadrupole time-of-flight mass spectrometry (UHPLC-QTOFMS; data not shown) and NMR analysis (Supplemental Fig. S3). Surprisingly, analysis of these compounds in whole-tissue extracts did not reveal major differences between mock- and aphid-infested plants (Fig. 2). However, defense-related proteins and metabolites often accumulate in the apoplast of stressed tissues, and the aphid stylet must pass through the spaces between the epidermal and mesophyll cells to reach the phloem. We, therefore, considered the possibility that *Bx1*-dependent resistance against aphids depends on extracellular accumulation of active BX compounds. Indeed, targeted HPLC analysis of apoplastic leaf extracts revealed a statistically significant increase of DIMBOA-glc and DIMBOA at 48 h of feeding (Fig. 2B). HDMBOA-glc levels were also increased in apoplastic leaf extracts from *R. padi*-infested plants, although this effect was more variable and borderline statistically significant (Student's *t* test; $P = 0.051$; Fig. 2B). Together, these results indicate that infestation by *R. padi* boosts BX accumulation in the apoplast.

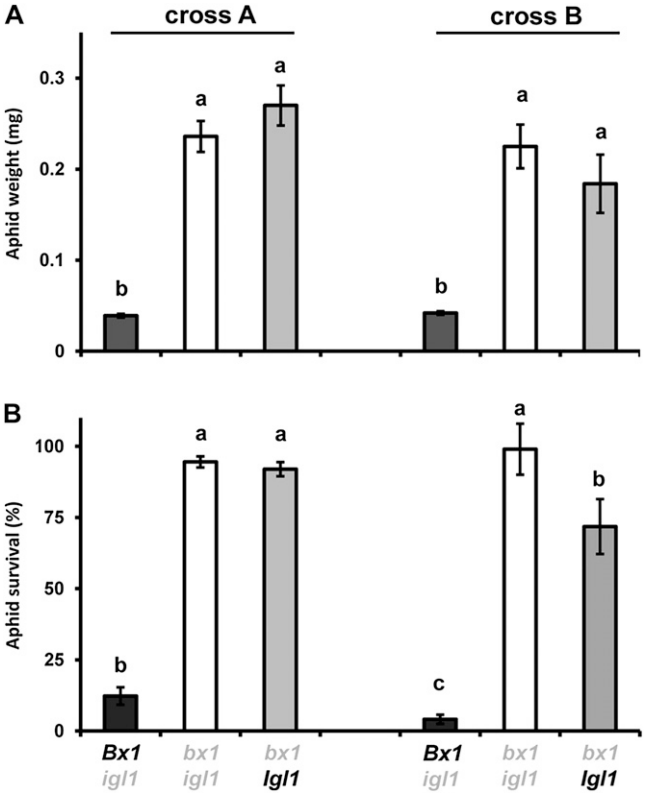


**Figure 1.** Contribution of *Bx1* and *Igl* to basal resistance against the cereal aphid *R. padi*. Batches of neonate nymphs in clip cages were allowed to feed for 7 d from the first leaf of *igl* mutant lines, *bx1* mutant lines, and *bx1 igl* double mutant lines, which had been selected from two independent crosses between the *bx1* mutant and *igl* mutant of maize. A, Average weights (±SEM; $n = 15$) of neonate nymphs after 7 d. B, Average percentages of batch survival (±SEM) after 7 d. Different letters indicate statistically significant differences (ANOVA, followed by Fisher's LSD test; $\alpha = 0.05$). Wild-type alleles are indicated in black and mutant alleles in gray. The comparison between *igl* and *bx1 igl* mutant lines was repeated in two additional experiments with similar results.

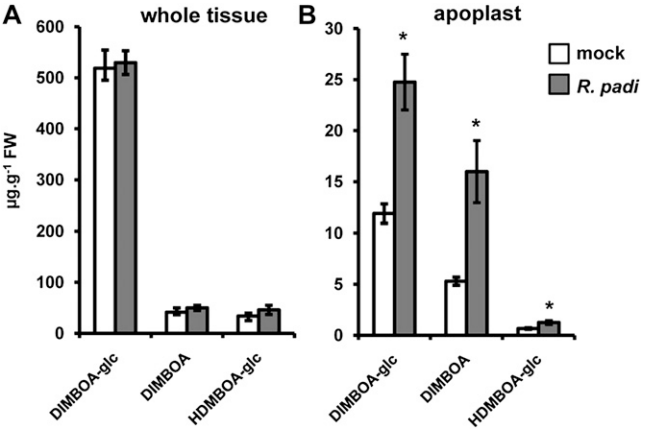


**Figure 2.** HPLC-DAD quantification of DIMBOA-glc, DIMBOA, and HDMBOA-glc in whole-tissue extracts (A) and apoplastic extracts (B) from mock- and *R. padi*-infested maize leaves. Material was collected at 48 h after aphid feeding in clip cages. Mock treatments consisted of clip cages without aphids. Data represent mean values in $\mu g\ g^{-1}$ fresh weight (±SEM) from four biologically replicated leaf samples. Asterisks indicate statistically significant differences compared to mock-treated leaves (Student's *t* test; $\alpha = 0.05$). The experiment was repeated with similar results.

### *Bx1* Contributes to Penetration Resistance against the Necrotrophic Fungus *S. turcica*

To study the role of BXs in resistance against pathogens, we quantified levels of colonization by the fungus *S. turcica* in leaves of *Bx1* wild-type lines (*Bx1 igl*) and *bx1* mutant lines (*bx1 igl* and *bx1 Igl*). This heminecrotrophic fungus penetrates the leaf tissue directly and colonizes the leaf apoplast before inducing necrosis (Agrios, 1997; Chung et al., 2010). *S. turcica*-inoculated leaves were collected at 3 d post inoculation (dpi), stained with lactophenol trypan blue, and examined for hyphal growth by light microscopy. In the progenies from both crosses, BX-deficient lines carrying the *bx1* mutant alleles allowed significantly more hyphal growth than the BX-producing lines carrying the *Bx1* wild-type alleles (Fig. 3A). This difference in resistance was also reflected by the fraction of arrested spores in the epidermal cell layer, which ranged between 14% and 23% in *bx1* mutant lines, to 47% and 49% in *Bx1* wild-type lines (Fig. 3B). Although the indole-producing *bx1* lines from both crosses expressed marginally higher levels of resistance than the indole-deficient double mutant lines, this difference was not statistically significant ($0.3 < P < 0.05$). Hence, *Bx1* contributes to slowing down and/or arresting *S. turcica* colonization during the relatively early stages of infection, whereas the defensive contribution of *Igl* appears marginal at this stage.

### *S. turcica* Elicits Apoplastic BX Accumulation during Early Stages of Infection

Based on our finding that *Bx1*-expressing plants express enhanced penetration resistance against *S. turcica*, we profiled levels of DIMBOA-glc, DIMBOA, and HDMBOA-glc from mock and *S. turcica*-inoculated wild-type plants. At the relatively early stage of 2 dpi, whole-tissue extracts from *S. turcica*-infected plants showed statistically increased levels of DIMBOA in comparison to mock-inoculated plants, whereas DIMBOA-glc and HDMBOA-glc remained similar between both treatments (Fig. 4A). As observed during the interaction with *R. padi* (Fig. 2A), apoplastic extracts from *S. turcica*-infected leaves showed a more dramatic response and contained significantly enhanced amounts of DIMBOA-glc, DIMBOA, and HDMBAO-glc compared to mock-inoculated leaves (Fig. 4B). By 5 dpi, BX profiles from *S. turcica*-infected leaves had changed, which coincided with the occurrence of disease symptoms. At this stage, *S. turcica*-inoculated leaves still produced more HDMBOA-glc than mock-inoculated leaves, but there was no longer a difference in DIMBOA-glc (Fig. 4). DIMBOA showed an even more dramatic increase than HDMBOA-glc, but was also more variable and not statistically significant in

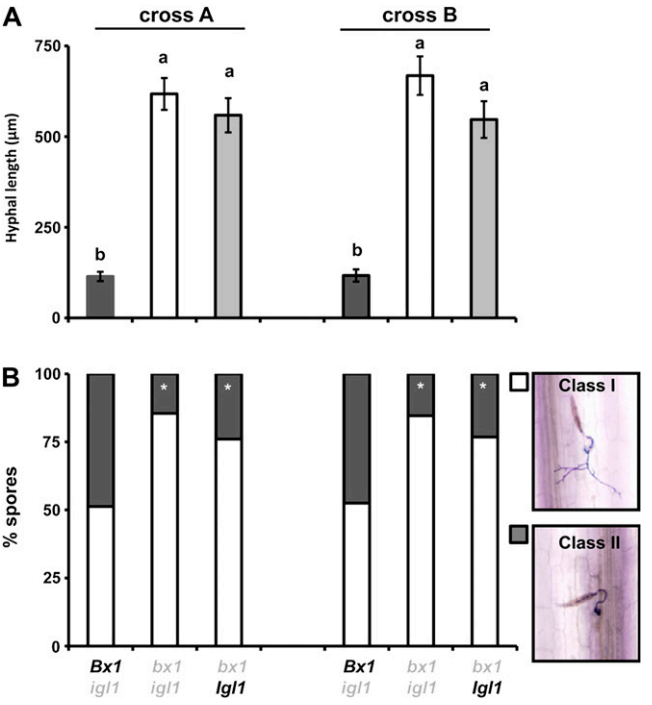


**Figure 3.** Contribution of *Bx1* and *Igl* to penetration resistance against the necrotrophic fungus *S. turcica*. Leaves of *igl* mutant lines, *bx1* mutant lines, and *bx1 igl* double mutant lines were inoculated with $5 \times 10^4$ spores $mL^{-1}$ and 3 d later collected for lactophenol trypan blue staining and microscopy analysis. A, Average hyphal lengths ($\mu$m) emerging from fungal spores (±SEM) in the epidermal cell layer. Different letters indicate statistically significant differences (ANOVA, followed by Fisher's LSD test; $\alpha = 0.05$; $n = 16$). B, Frequency distributions between developing germination hyphae (class I; white) and arrested germination hyphae (class II; gray). Asterisks indicate statistically significant differences compared to BX-producing *igl* mutant lines from each cross ($\chi^2$ test; $\alpha = 0.05$; $n = 16$). The comparison between *igl* and *bx1 igl* mutant lines was repeated in two additional experiments with similar results.

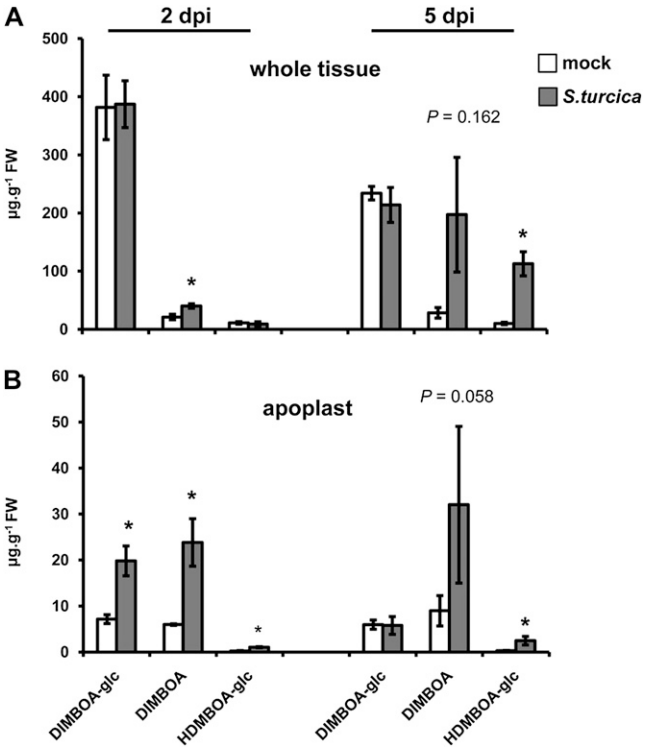


**Figure 4.** HPLC-DAD quantification of DIMBOA-glc, DIMBOA, and HDMBOA-glc in whole-tissue extracts (A) and apoplastic extracts (B) from mock- and *S. turcica*-inoculated maize leaves. Material was collected at 2 and 5 dpi. Data represent means in $\mu g\ g^{-1}$ fresh weight (±SEM) from three biologically replicated samples. Asterisks indicate statistically significant differences compared to mock-treated leaves (Student's *t* test; $\alpha = 0.05$). *P* values indicate levels of statistical significance.

comparison to mock-treated leaves (Fig. 4). Hence, maize deposits increased levels of DIMBOA-glc, DIMBOA, and HDMBOA-glc in the apoplast during the relatively early stages of *S. turcica* infection, and continues to accumulate HDMBOA-glc and DIMBOA during later symptomatic stages of the interaction.

### DIMBOA Regulates Transcriptional Feedback Inhibition of BX Biosynthesis

To elucidate further the involvement of the BX pathway in maize innate immunity, we profiled BX production and *Bx* gene expression after leaf infiltration with chitosan, a PAMP that is common in fungal cell walls and insect shells (Iriti and Faoro, 2009). At 24 h after infiltration with chitosan, whole-tissue extracts showed increased levels of HDMBOA-glc in comparison to mock-treated leaves (Fig. 5A). Apoplastic extracts from chitosan-treated leaf segments displayed a more pronounced increase in DIMBOA and HDMBOA-glc (Fig. 5B), thereby resembling the BX response to *R. padi* or *S. turcica*. Surprisingly, however, reverse-transcriptase quantitative PCR (RT-qPCR) analysis of *Bx* gene expression revealed reduced expression of *Bx4*, *Bx5*, *Bx6*, *Bx7*, *Bx8*, and *Bx9* after treatment with chitosan (Fig. 6A). To investigate whether this transcriptional repression is due to negative feedback inhibition from BX compounds, we profiled *Bx* gene expression after exposure to the volatile BX precursor indole. As is shown in Figure 6B, indole triggered comparable patterns of *Bx* gene repression as chitosan. Furthermore, comparison of *Bx* gene transcription between BX-producing *igl* single mutant lines and BX-deficient *bx1 igl* double mutant lines revealed enhanced *Bx* expression in BX-deficient plants (Fig. 6, C and D), providing further genetic evidence for transcriptional feedback inhibition by BXs. Since chitosan boosts accumulation of both DIMBOA and HDMBOA-glc in the apoplast (Fig. 5B), we purified DIMBOA and HDMBOA-glc by preparative HPLC and examined which of both compounds is responsible for the feedback response. At 24 h after infiltration of the purified compounds in the leaf apoplast, DIMBOA repressed *Bx* gene expression in a dose-dependent manner (Fig. 6, E and F), whereas HDMBOA-glc had no statistically significant effect (Fig. 6G). We, therefore, conclude that DIMBOA acts as an extracellular signal for transcriptional feedback of BX biosynthesis.

### DIMBOA Regulates Callose Deposition

PAMP-induced callose deposition is commonly used as a marker for plant innate immunity (Luna et al., 2011). Chitosan elicits callose deposition in a wide variety of plants (Iriti and Faoro, 2009). To optimize this PAMP response in maize, we quantified callose after leaf infiltration with increasing concen-

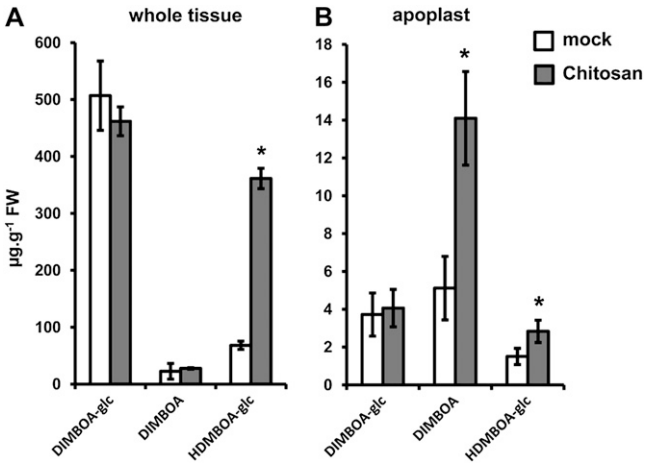


**Figure 5.** HPLC-DAD quantification of DIMBOA-glc, DIMBOA, and HDMBOA-glc in whole-tissue extracts (A) and apoplastic extracts (B) at 24 h after infiltration of leaf segments with 0.2% chitosan or mock buffer. Data represent means in $\mu g\ g^{-1}$ fresh weight (±SEM) from three biologically replicated samples. Asterisks indicate statistically significant differences compared to mock-treated leaves (Student's *t* test; $\alpha = 0.05$). The experiment was repeated twice with similar results.

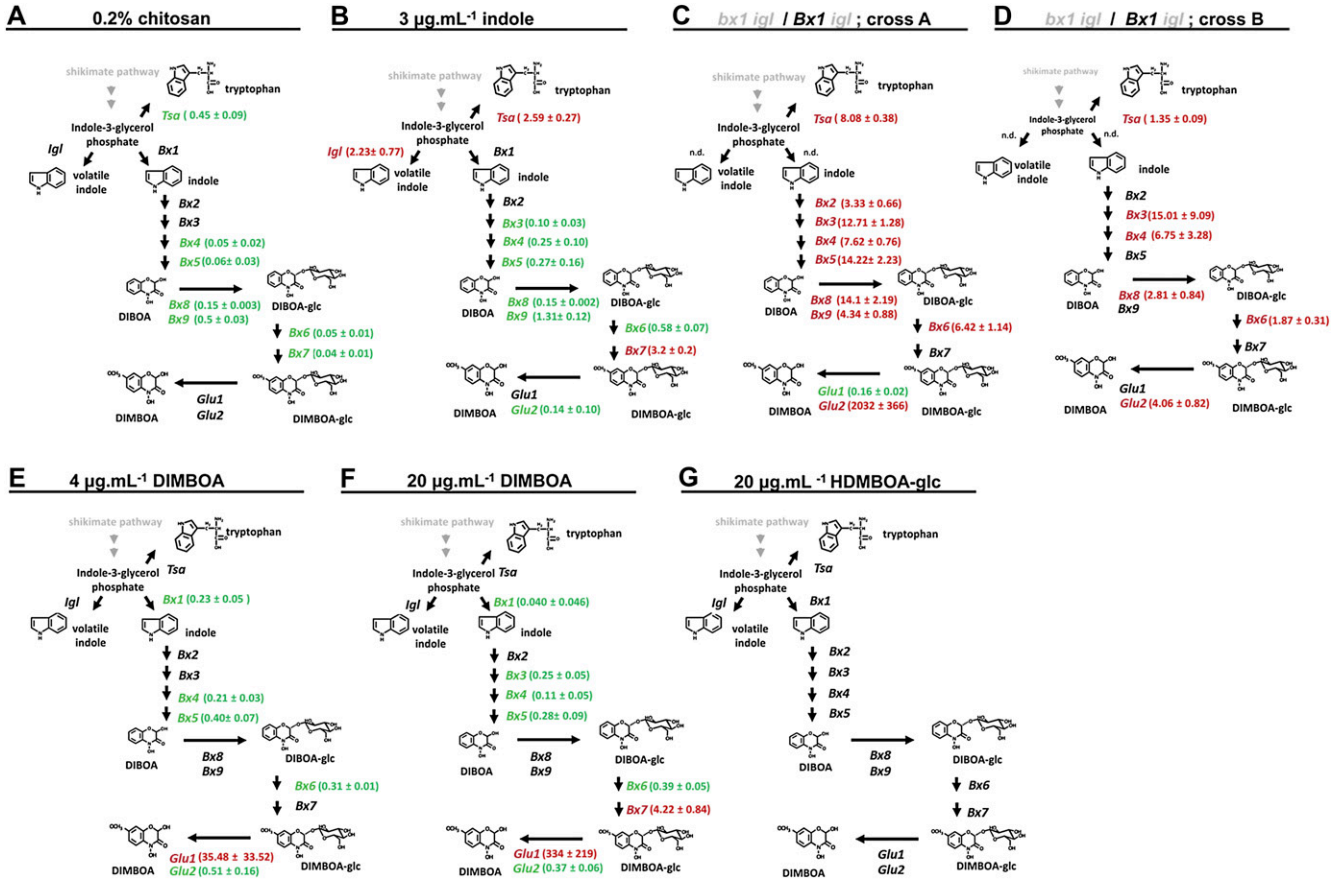


**Figure 6.** Transcriptional feedback regulation of the BX pathway by DIMBOA. Apoplastic infiltration with BX-inducing concentrations of chitosan (0.2%; A) and exposure to the volatile BX precursor indole (B) repressed *Bx* gene expression. BX-deficient *bx igl* double mutant lines displayed enhanced *Bx* gene transcription compared to BX-producing *igl* single mutant lines (C and D). Apoplastic leaf infiltration with DIMBOA (E and F) repressed *Bx* gene expression, whereas HDMBOA-glc had no effect (G), suggesting transcriptional feedback regulation by apoplastic DIMBOA. Shown are average fold-change values (±SEM) of genes with a statistically significant level of induction (red) or repression (green) compared to mock treatments (A, B, E, and G) or BX-producing *igl* single mutant lines (C and D). Differences in expression between three biologically replicated samples from independent experiments were tested for statistical significance, using Student's *t* tests or a nonparametric Wilcoxon-Mann-Whitney test when values did not follow normal distributions ($\alpha = 0.05$). n.d., Not determined.

trations of chitosan. At 24 h after infiltration, maize leaves deposited callose in a dose-dependent manner (Supplemental Fig. S4), confirming that chitosan-induced defense is marked by callose deposition in maize. In Arabidopsis, PAMP-induced callose requires endogenous production of indolic GSs (Clay et al., 2009), suggesting a signaling function by these secondary metabolites. Since monocots do not produce indolic GSs, we tested whether BXs fulfill a similar role in maize innate immunity. To this end, we treated leaves with nonsaturating concentrations of chitosan (0.05%) and assayed callose deposition in leaves of BX-producing *Bx1 igl* lines and BX-deficient *bx1 igl* lines. This experiment revealed that the BX-deficient lines deposit significantly lower amounts of callose than the BX-producing lines after treatment with chitosan (Fig. 7). Hence, PAMP-induced callose requires regulation by one or more *Bx1*-dependent metabolites. Since chitosan increases DIMBOA and HDMBOA-glc in the apoplast (Fig. 5), we examined which of these two compounds are responsible for *Bx1*-dependent callose. To this end, we quantified callose intensities at 24 h after apoplast infiltration with either of both compounds. As observed for *Bx* gene repression (Fig. 6), DIMBOA was active and triggered callose deposition in a dose-dependent manner, whereas HDMBOA-glc was inactive and failed to boost callose deposition (Fig. 8). Hence, DIMBOA functions as an extracellular signal for PAMP-induced callose.

## DISCUSSION

The role of BXs in plant defense against pests and diseases has been studied for decades. Most of these studies are based on either in vitro evidence, where BX compounds had been supplemented to artificial growth medium, or on correlative evidence between resistance

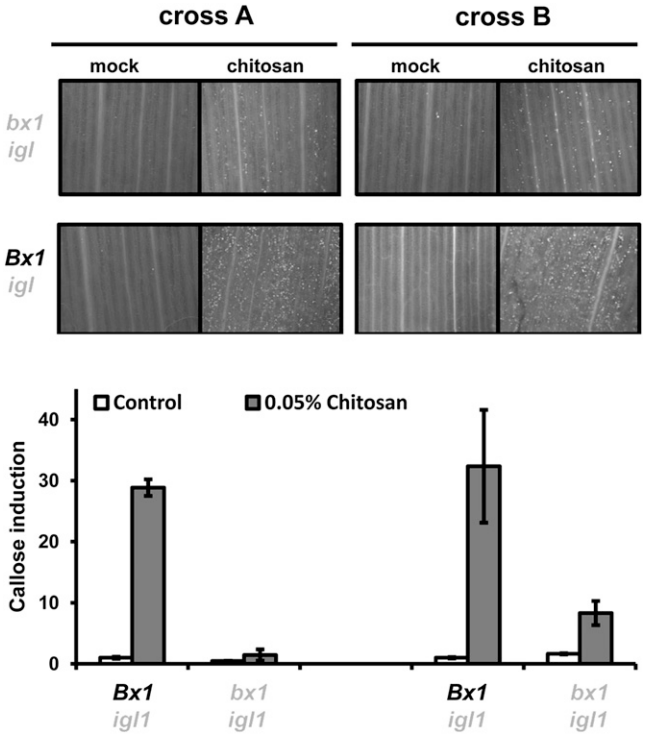


**Figure 7.** *Bx1* regulates chitosan-induced callose deposition. Leaf segments from *igl* single mutant lines and *bx1 igl* double mutant lines were infiltrated with chitosan (0.05%) or mock solution. At 24 h after infiltration, leaf segments were collected for aniline blue staining, UV-epifluoresence microscopy, and digital quantification of callose intensity. Shown are fold-induction values of callose (±SEM; $n = 15$), relative to the average callose intensity in mock-treated *Bx1 igl* lines from each cross. Photographs show representative differences in fluorescent callose signals under UV-epifluoresence microscopy.

and BX levels among cereal varieties and/or inbred lines (for review, see Niemeyer, 1988, 2009). For instance, in vitro supplied DIMBOA has been demonstrated to affect a broad spectrum of herbivorous insects and microbes, including aphids (Cambier et al., 2001) and *S. turcica* (Rostás, 2007). Other studies revealed negative correlations between endogenous BX concentrations and aphid performance in populations of cereal varieties (Argandoña et al., 1980; Leszczynski and Dixon, 1990; Niemeyer and Perez, 1994). In this study, we have investigated the defense function of BXs further, by comparing resistance phenotypes of wild-type and *bx1* maize lines in the background of the *igl* mutant. Since IGL controls herbivore-induced indole production, the *igl* mutation prevents production of IGL-dependent BXs and, therefore, allows for a more accurate assessment of the defense contribution by BXs against IGL-inducing pests and diseases. Comparison between BX-producing and BX-deficient progenies from two independent crosses between the *igl* mutant and the *bx1* mutant confirmed a major role for BXs in resistance against the cereal aphid *R. padi* (Fig. 1). Using these lines, we also discovered a significant contribution of BXs to early acting penetration resistance against the necrotophic fungus *S. turcica* (Fig. 3). Hence, BXs play an important role in basal resistance against aphids and fungi. Interestingly, the expression of this BX-dependent resistance occurred before the occurrence of large-scale tissue disruption or symptom development.

The involvement of BXs in penetration resistance against *S. turcica* (Fig. 3B) suggests an alternative mode of action that contradicts the classical notion that BX defense requires tissue damage to hydrolyze vacuole-localized BX-glc compounds by plasmid-localized $\beta$-glucosidases (Morant et al., 2008). Chromatographic profiling of BX compounds revealed increased accumulation of apoplastic DIMBOA-glc, DIMBOA, and HDMBOA-glc during the relatively early stages of infestation by either *R. padi* or *S. turcica* (Figs. 2 and 4). Notably, during both interactions, these effects preceded major tissue disruption or symptom development. Since aphid stylets and fungal hyphae must colonize the host apoplast before the host-parasite interaction can be established, enhanced deposition of biocidal BXs in this compartment is consistent with a role in penetration resistance. Based on our findings, we propose an alternative mode of BX-dependent defense, which depends on the accumulation of DIMBOA-glc and HDMBOA-glc into the apoplast, where they contribute to penetra-

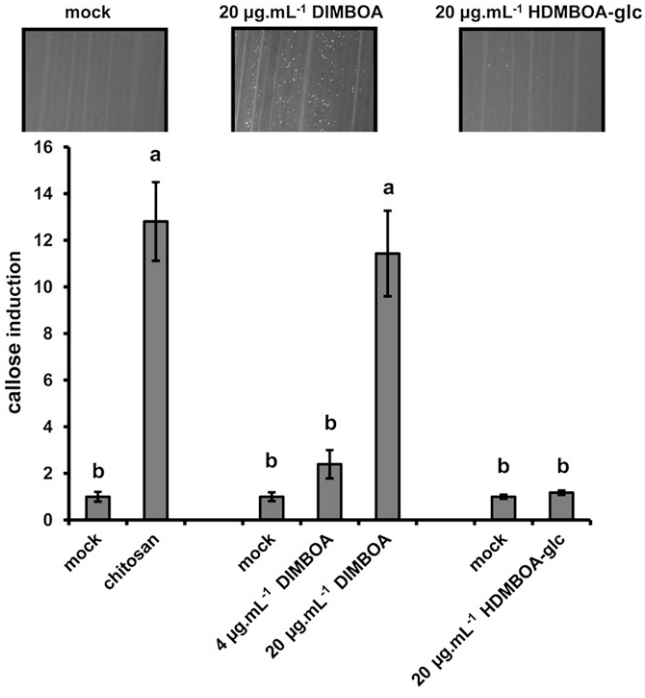


**Figure 8.** DIMBOA-induced callose deposition. Infiltration with 20 $\mu$g mL$^{-1}$ DIMBOA elicits similar levels of callose deposition as infiltration with chitosan (0.1%), whereas infiltration with 20 $\mu$g mL$^{-1}$ HDMBOA-glc had no effect in comparison to the corresponding mock treatment. Shown are fold-induction values of callose deposition (±SEM; $n = 15$), relative to average callose intensities in mock treatments at 24 h after infiltration treatment. Different letters indicate statistically significant differences (ANOVA, followed by Fisher's LSD test; $\alpha = 0.05$). Photographs show representative differences in fluorescent callose signals by UV-epifluorescence microscopy.

tion resistance upon subsequent activation by plant- or attacker-derived β-glucosidases (Fig. 9). In support of this, we observed increased accumulation of DIMBOA aglycone in the apoplast of challenged leaves (Figs. 2 and 4). The lack of HDMBOA aglycone in this fraction can be explained by the highly unstable nature of this metabolite (Maresh et al., 2006). Although we cannot exclude that apoplastic BX accumulation during the early stages of aphid or fungal infestation occurs entirely without tissue damage, our experiments with chitosan demonstrate that this response can occur independently of tissue damage in maize. The mock treatments of these experiments involved a similar leaf infiltration as the chitosan treatments, but failed to increase apoplastic BX content (Fig. 5). Hence, the difference in BX accumulation between both treatments is not triggered by possible tissue damage during leaf infiltration. Future research will be necessary to identify the molecular transportation mechanisms underpinning PAMP-induced BX accumulation in the apoplast.

In addition to the defensive contribution of *Bx1*, we were also able to determine the role of *Igl* by comparing resistance levels between indole-producing *bx1* single mutants and indole-deficient *bx1 igl* double mutants. Although aphid performance and fungal colonization were consistently lower in *Igl* wild-type lines compared to *igl* mutant lines, this difference was only statistically significant for aphid survival in the progeny from one cross, and was not proportional to the relatively major contribution from the *Bx1* allele (Fig. 1B). Nonetheless, these relatively weak effects by *Igl* suggest a minor contribution from IGL-derived BXs. It is possible that IGL has a more prominent contribution during the later stages of the interaction, when more IGL-derived indole is channeled into the BX pathway and replenishes the rapidly declining pool of DIMBOA-glc. The extent of this contribution requires further investigation and can be addressed by comparing BX profiles between indole-producing *Igl* lines and indole-deficient *igl* lines at different stages of the plant-parasite interaction. These lines will also prove useful to assess the role of IGL-dependent indole emission in tritrophic interactions and indirect defense against herbivores.

Early acting postinvasive plant defense is marked by a rapid accumulation of reactive oxygen species followed by deposition of callose-rich papillae (Ton et al., 2009; Luna et al., 2011). Our finding that *bx1* mutant lines are affected in PAMP-induced callose suggests a regulatory function of BXs in this defense response (Fig. 7). Recently, it was reported that DIMBOA acts as an electron acceptor for apoplastic cytokinin dehydrogenase, thereby contributing to the degradation of cytokinins (Frébortová et al., 2010). Since cytokinins can antagonize abscisic acid (ABA)-regulated plant processes (Shkolnik-Inbar and Bar-Zvi, 2010; Subbiah and Reddy, 2010; Vysotskaya et al., 2010), it is tempting to speculate that DIMBOA-catalyzed cytokinin degradation contributes to ABA-dependent priming of callose deposition (Ton et al., 2009). In support of this, we found that apoplast infiltration with DIMBOA boosts callose deposition (Fig. 8). Interestingly, Frébortová et al. (2010) proposed that DIMBOA-dependent degradation of cytokinins depends on the −N-OH group of DIMBOA at the indolic ring, which is absent in HDMBOA after *O*-methylation. Indeed, HDMBOA-glc failed to elicit callose deposition in our experiments (Fig. 8). Future research will be necessary to decipher the interplay between extracellular DIMBOA, cytokinins, and

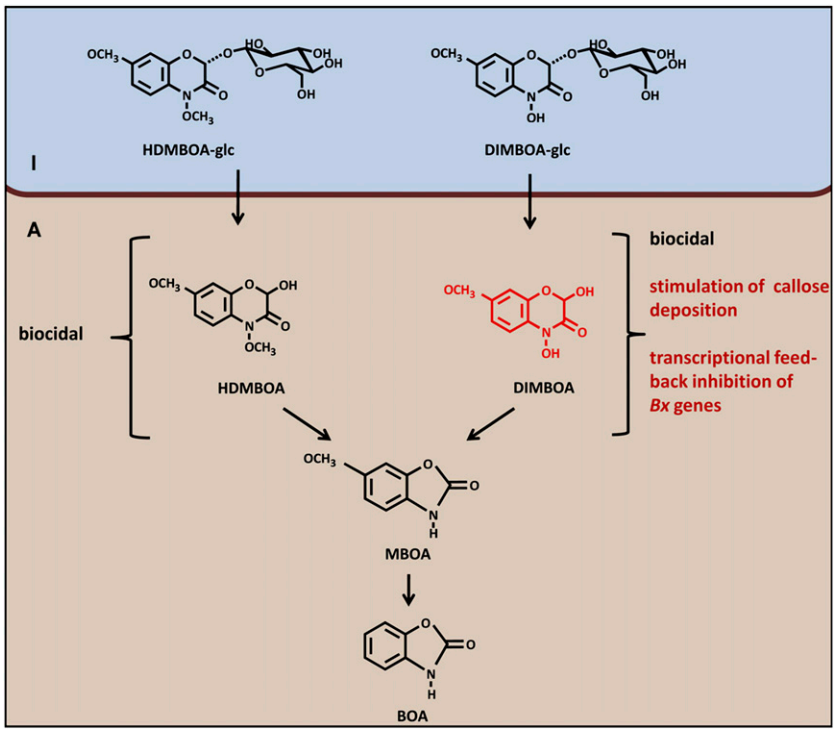


**Figure 9.** Model of BX-dependent innate immunity against aphids and fungi. Activation of maize innate immunity leads to apoplastic deposition of HDMBOA-glc and DIMBOA-glc. Subsequent hydrolysis into biocidal aglycones can provide chemical defense against pests and diseases (Cambier et al., 2001; Rostás, 2007). Both HDMBOA and DIMBOA are degraded into MBOA and BOA (Maresh et al., 2006), indicating that DIMBOA (red), and not HDMBOA, has an additional function in the regulation of *Bx* gene expression and callose deposition. I, Intracellular space; A, apoplast.

ABA in the regulation of postinvasive cereal defense against pests and diseases.

PAMP-induced callose in Arabidopsis requires intact biosynthesis of the 4-methoxylated indolic GS 4MI3G and subsequent hydrolysis by the atypical myrosinase PEN2 (Clay et al., 2009). This discovery revealed an important regulatory function of breakdown products of indolic GSs in Arabidopsis innate immunity, but at the same time raised the question how non-Brassicaceous plants regulate callose deposition. In this study, we have examined whether BXs fulfill a similar regulatory function in maize, and found that BX-deficient *bx1* lines are indeed dramatically reduced in their capacity to deposit PAMP-induced callose compared to BX-producing *Bx1* lines (Fig. 7). Moreover, of the two chitosan-inducible BXs, only DIMBOA elicited callose deposition upon infiltration into the apoplast, whereas infiltration with similar amounts of HDMBOA-glc failed to trigger callose depositions (Fig. 8). A similar compound specificity was found for the transcriptional feedback regulation of the BX pathway (Fig. 6). Since DIMBOA and HDMBOA-glc are both degraded into MBOA and BOA (Maresh et al., 2006; Macías et al., 2007), it can be concluded that extracellular DIMBOA, rather than its successive breakdown products, is responsible for the regulation of callose deposition and *Bx* gene expression (Fig. 9). We, therefore, hypothesize that this signaling function originates from a conserved detoxification response, which prevents autotoxic buildup of BXs by translocation to the apoplast. Once deposited into the apoplast, BX-glucosides become hydrolyzed and captured in a matrix of callose to provide targeted chemical defense against invading parasites. The striking analogy with indolic GS metabolites in Arabidopsis points to a conserved regulatory function of indole-derived secondary metabolites in innate immunity across the plant kingdom.

## CONCLUSION

BX-deficient maize is more susceptible to aphids and is affected in penetration resistance against fungal pathogens. The difference in resistance between BX-deficient and BX-producing maize lines occurs before the onset of major tissue damage and manifests itself as increased accumulation of BX compounds in the apoplast. In addition to its contribution as a biocidal defense metabolite, extracellular DIMBOA regulates *Bx* gene expression and PAMP-induced callose, which reveals a novel regulatory function of BX metabolites in cereal innate immunity against pests and diseases.

## MATERIALS AND METHODS

### Plant Material and Cultivation

The Pioneer Hi-Bred collection of 42,300 F1 maize (*Zea mays*) plants, mutagenized by means of Robertson's *Mu* element, was screened for *Mu*-containing alleles of *Igl* by a reverse-genetics approach (Bensen et al., 1995). PCR amplification was performed as described previously (Mena et al., 1996). *Mu* integration in the nontranslated 5′-leader region of *Igl* was identified and Mendelian segregation was confirmed within the progeny. Heterozygous progeny was selfed from which one homozygous mutant was identified (cv B73). This plant was used as female (cross 307) and male (cross 308), respectively, in crosses with the homozygous *bx1* reference allele mutant (cv GeHu Yellow Dent; Hamilton, 1964). Individual heterozygous progeny (plants 308-1, 308-5, and 307-1) of the two reciprocal crosses were used to generate segregating progeny for the wild-type and mutant alleles of *Bx1* and *Igl*. Homozygous lines 22 (*bx1 igl*), 7 (*bx1 Igl*), and 25.13 (*Bx1 igl*) were selected from a cross between 308-1 × 307-1 (cross A), whereas lines 32R (*bx1 igl*), 16R (*bx1 Igl*), and 24R (*Bx1 igl*) were selected from a cross between 308-5 × 307-1 (cross B). Genotypes from these crosses were initially identified by phenotyping (*bx1bx1* mutants; $FeCl_3$ root staining; Bailey and Larson, 1991), or PCR genotyping (*igl* mutants), and were propagated by selfing. Resulting F3 and F4 lines were further selected and confirmed by HPLC-DAD analysis of BX leaf content and gas chromatography-MS analysis of indole emission from *Spodoptora littoralis*-infested or wounded plants as described previously (Ton et al., 2007; Supplemental Fig. S1). Plant responses to *Rhopalosiphum padi*, *Setosphaeria turcica*, chitosan, indole, DIMBOA, or HDMBOA-glc were performed with the BX- and indole-producing wild-type cv Delprim (Delley Semences). Seeds were germinated at 22°C in petri dishes in the dark. After 2 to 3 d, germinated seedlings of similar size were transplanted to pots containing compost soil and cultivated under controlled conditions (16:8 h light:dark [L:D], 22°C).

### Aphid and Fungus Bioassays

*R. padi* were obtained from a single field-collected apterous virginopara, reared under controlled conditions (16:8 h L:D, 22°C) on maize (cv Delprim) for at least 10 generations. No-choice development assays were performed by placing 15 replicated groups of six adult apterae in clip cages, attached to the first leaf of 8-d-old plants, and left overnight to larviposit. The adult apterae were then removed and neonate nymphs were counted. A maximum of 10 nymphs per clip cage were retained. For each assay, seedlings were maintained in a controlled climate chamber for 6 d (20°C ± 2°C, 16:8 h L:D, 40% relative humidity) after which surviving nymphs were counted and then weighed in their batches in a 0.2-mL microfuge tube on a microbalance (Cahn C33, Scientific and Medical Products Ltd.). Data were expressed as average weight per aphid or as percentage of aphid survival, and subjected to ANOVA. To determine aphid-induced BX production, at least 10 replicated batches of 25 late instar nymphs were enclosed in clip cages on 8-d-old plants and left to feed for 48 h. Aphids were then removed and leaf tissues were extracted as described below. Mock-treated plants had clip cages only. For HPLC analysis of BX content, leaf material was collected from four to six infested leaves from different plants. *S. turcica* cultivation, spore collection, and inoculation of 8-d-old seedlings ($5 \times 10^4$ spores $mL^{-1}$) were performed as described by Rostás et al. (2006). Sixteen randomly collected segments (2–3 cm) from inoculated leaves of four different plants per line were collected at indicated time points and divided for HPLC analysis and microscopic analysis following trypan blue lactophenol blue staining (Koch and Slusarenko, 1990). Colonization by *S. turcica* was examined microscopically. Penetration resistance was expressed as the fraction of arrested spores, or the average hyphal length emerging from germinating spores, which was determined from digital photographs, using ImageJ software (http://rsb.info.nih.gov/ij/index.html).

### BX Extraction, Quantification and Verification

BX extraction and analysis by HPLC-DAD were adapted from Baumeler et al. (2000). Briefly, weighed plant material was frozen in liquid nitrogen and pulverized by vortexing in microfuge tubes containing four ball bearings (3 mm Ø). After addition of 1-mL extraction buffer (EB; methanol/acetic acid (HAc); 49/1; v/v), samples were sonicated (10 min) and centrifuged (12,600*g*, 10 min). Supernatants were collected for analysis by a Shimadzu prominence HPLC system (Shimadzu Corporation) with BetaSil C18 column (250 mm × 4.6 mm; 5 $\mu$ particle size; Thermo Scientific) and diode array detector set at 254 nm. The mobile phase consisted of a mixture of pure water (solution A) and methanol/isopropanol/HAc (3,800/200/1; v/v; solution B). The flow rate was maintained at 1 mL $min^{-1}$, starting with isocratic conditions at 10% B for 2 min, linear gradient to 50% B from 2 to 27 min, isocratic conditions at 50% B from 27 to 29 min, linear reverse gradient to 10% B from 29 to 31 min, and isocratic conditions at 10% B from 31 to 35 min. Retention times of the different BXs were established from synthetic standards (kindly provided by Prof.

Dieter Sicker, University of Leipzig). BX tissue content ($\mu$g $g^{-1}$ fresh weight) was estimated from standard curves, which showed linear relationships between peak area and concentration. Mass identities of DIMBOA-glc, DIMBOA, and HDMBOA-glc were confirmed by UHPLC-QTOFMS (data not shown). Since DIMBOA and HDMBOA-glc elute closely together using the above HPLC separation protocol, we performed additional verification of both compounds by NMR analysis after preparative HPLC purification. $^1$H, gradient correlation spectroscopy and gradient heteronuclear single quantum coherence spectra were recorded with a Varian VNMRS 500 MHz spectrometer; the chemical shifts were reported in ppm from tetramethylsilane with the residual solvent resonance taken as the internal standard. For DIMBOA, the $^1$H-NMR spectrum revealed five resonances (Supplemental Fig. S3A), which were readily assigned to the $OCH_3$, aliphatic CH, and three aromatic CH groups. For HDMBOA-glc, six proton resonances from the aglycone framework (Supplemental Fig. S3B) were detected whereas proton resonances from the glycoside moiety were observed as broad singlets or multiplets with chemical shifts comparable to closely related glycosides (Rashid et al., 1996). $^1$H-$^1$H gradient correlation spectroscopy and single-bond $^1$H-$^{13}$C gradient heteronuclear single quantum coherence experiments were used to further confirm the identity of the HDMBOA-glc (data not shown). Although BX compounds can be unstable during extraction procedures, our extraction method yielded recovery rates of >98% when purified BX compounds were added to plant tissues before grinding.

## Extraction of Apoplastic Fluids

The method was adapted from Yu et al. (1999) and Boudart et al. (2005). Briefly, collected leaf tissues were weighted and submerged into 14 $\mu$g $mL^{-1}$ proteinase K solution (Sigma) under a glass stopper in Greiner tubes. Vacuum infiltration was performed using a desiccator at −60 kPa for 5 min. After infiltration, leaf tissues were blotted dry, carefully rolled up, and placed in a 12-mL tubes, containing 20 ball bearings (3 mm Ø) and 0.5 mL EB supplemented with 14 $\mu$g $mL^{-1}$ proteinase K. After centrifugation for 5 min at 2.300*g* (4°C), tissues were removed and the collected liquid comprising EB and apoplastic fluid was collected from beneath the ball bearings with a pipette and subjected to HPLC analysis. Leaf segments infiltrated with chitosan solution were incubated for 24 h in sealed petri dishes before centrifugation.

## Chemical Treatments and Callose Quantification

Indole exposure was performed with 10-d-old plants of similar size. Plants ($n$ = 9) per treatment were placed in air-tight glass chambers and exposed to indole that had been dissolved in dichloromethane, or dichloromethane only (mock), applied on filter paper discs. After 24 h of exposure, leaf segments (2–3 cm) from the second leaf were collected and divided for analysis of gene expression and BX content. Analyses of gene expression, BX content, and callose deposition after chemical leaf infiltration were based on nine to 18 randomly collected leaf segments (2–3 cm; second leaf) from at least three different 10-d-old plants per treatment. Chitosan (Sigma) was dissolved to 1% (m/v) in 1% HAc initially, and diluted to 0.2% chitosan (0.2% HAc) with water. Subsequent dilutions to 0.1% or 0.05% chitosan were performed with 0.2% HAc, and adjusted to pH = 5.5 to 5.7. Chitosan solutions were infiltrated in leaf segments (2–3 cm) as described above, and left for 24 h under standard growth conditions before further analysis. Mock treatments were performed similarly with 0.2% HAc (pH = 5.5–5.7). DIMBOA and HDMBOA-glc were purified using a semipreparative BetaSil C18 column (250 mm × 10 mm; 5 $\mu$ particle size; Thermo Scientific) at a flow rate of 4 mL $min^{-1}$. Collected elutes were lyophilized and resuspended in EB. After verification by HPLC-DAD and UHPLC-QTOFMS, compounds were diluted to indicated concentrations (1.96% methanol; 0.04% HAc; pH 5.5–5.7), and infiltrated into leaf segments, as described above. Mock treatments were performed similarly using 1.96% methanol 0.04% HAc (pH = 5.5–5.7). Aniline blue staining and quantification of callose by epifluorescence microscopy were performed, as described by Luna et al. (2011).

## RNA Isolation, cDNA Preparation, and RT-qPCR Analysis

Gene expression analyses were based on three biologically replicated samples from the second leaf of 10-d-old plants. Total RNA was extracted as described previously (Matthes et al., 2010). Genomic DNA was digested according to manufacturer's guidelines (RQ1 RNase-Free DNase; Promega). Synthesis of cDNA was performed as described by Ton et al. (2007). Two technical replicates of each cDNA sample were subjected to RT-qPCR analysis, as described previously (Ahmad et al., 2011). Primer sequences are listed in Supplemental Table S1. PCR efficiencies ($E$) of primer pairs were estimated from multiple amplification plots using the equation $(1 + E) = 10^{slope}$ (Ramakers et al., 2003), and were confirmed to provide $(1 + E)$ values close to 2. Transcript levels were calculated relative to the reference genes *GAPC* or *Actin-1* (Erb et al., 2009), using the $2^{\Delta\Delta Ct}$ method, as described (Livak and Schmittgen, 2001; Schmittgen and Livak, 2008), or the $2^{\Delta Ct}$ method, where $\Delta Ct$ = Ct (reference gene) − Ct (gene of interest).

## Supplemental Data

The following materials are available in the online version of this article.

**Supplemental Figure S1.** Confirmation of mutant phenotypes of *bx1* and *igl* carrying maize lines.

**Supplemental Figure S2.** HPLC-DAD quantification of basal and chitosan-induced DIMBOA-glc, DIMBOA, and HDMBOA-glc in whole-leaf extracts from the *igl* single mutant, the *bx1* single mutant, and the *bx1 igl* double mutant (cross B).

**Supplemental Figure S3.** $^1$H-NMR spectrogram of DIMBOA (A) and HDMBOA-glc (B).

**Supplemental Figure S4.** Dose-dependent callose deposition at 24 h after pressure infiltration with different concentrations of chitosan.

**Supplemental Table S1.** Primers used for RT-qPCR analysis of gene expression.

## ACKNOWLEDGMENTS

We thank Ted Turlings for critically proofreading an earlier version of this manuscript. We also thank the technical support from Servei Central d'Instrumentació Científica, University of Jaume I, and Cristian Barrera for assistance with the NMR analysis.

Received May 27, 2011; accepted June 30, 2011; published July 5, 2011.

## LITERATURE CITED

**Agrios GN** (1997) Plant Pathology, Ed 4. Academic Press Inc., San Diego

**Ahmad S, Van Hulten M, Martin J, Pieterse CM, Van Wees SCM, Ton J** (2011) Genetic dissection of basal defence responsiveness in accessions of *Arabidopsis thaliana*. Plant Cell Environ **34:** 1191–1206

**Argandoña VH, Luza JG, Niemeyer HM, Corcuera LJ** (1980) Role of hydroxamic acids in the resistance of cereals to aphids. Phytochemistry **19:** 1665–1668

**Bailey BA, Larson RL** (1991) Maize microsomal benzoxazinone N-monooxygenase. Plant Physiol **95:** 792–796

**Baumeler A, Hesse M, Werner C** (2000) Benzoxazinoids-cyclic hydroxamic acids, lactams and their corresponding glucosides in the genus *Aphelandra* (Acanthaceae). Phytochemistry **53:** 213–222

**Bednarek P, Pislewska-Bednarek M, Svatos A, Schneider B, Doubsky J, Mansurova M, Humphry M, Consonni C, Panstruga R, Sanchez-Vallet A, et al** (2009) A glucosinolate metabolism pathway in living plant cells mediates broad-spectrum antifungal defense. Science **323:** 101–106

**Bensen RJ, Johal GS, Crane VC, Tossberg JT, Schnable PS, Meeley RB, Briggs SP** (1995) Cloning and characterization of the maize *An1* gene. Plant Cell **7:** 75–84

**Boudart G, Jamet E, Rossignol M, Lafitte C, Borderies G, Jauneau A, Esquerré-Tugayé MT, Pont-Lezica R** (2005) Cell wall proteins in apoplastic fluids of *Arabidopsis thaliana* rosettes: identification by mass spectrometry and bioinformatics. Proteomics **5:** 212–221

**Cambier V, Hance T, De Hoffmann E** (2001) Effects of 1,4-benzoxazin-3-one derivatives from maize on survival and fecundity of *Metopolophium dirhodum* (Walker) on artificial diet. J Chem Ecol **27:** 359–370

**Chung C-L, Longfellow JM, Walsh EK, Kerdieh Z, Van Esbroeck G, Balint-Kurti P, Nelson RJ** (2010) Resistance loci affecting distinct stages

of fungal pathogenesis: use of introgression lines for QTL mapping and characterization in the maize—*Setosphaeria turcica* pathosystem. BMC Plant Biol **10:** 103

**Cicek M, Esen A** (1999) Expression of soluble and catalytically active plant (monocot) beta-glucosidases in *E. coli*. Biotechnol Bioeng **63:** 392–400

**Clay NK, Adio AM, Denoux C, Jander G, Ausubel FM** (2009) Glucosinolate metabolites required for an Arabidopsis innate immune response. Science **323:** 95–101

**Czjzek M, Cicek M, Zamboni V, Burmeister WP, Bevan DR, Henrissat B, Esen A** (2001) Crystal structure of a monocotyledon (maize ZMGlu1) beta-glucosidase and a model of its complex with p-nitrophenyl beta-D-thioglucoside. Biochem J **354:** 37–46

**D'Alessandro M, Held M, Triponez Y, Turlings TC** (2006) The role of indole and other shikimic acid derived maize volatiles in the attraction of two parasitic wasps. J Chem Ecol **32:** 2733–2748

**Delp G, Gradin T, Ahman I, Jonsson LM** (2009) Microarray analysis of the interaction between the aphid *Rhopalosiphum padi* and host plants reveals both differences and similarities between susceptible and partially resistant barley lines. Mol Genet Genomics **281:** 233–248

**Erb M, Flors V, Karlen D, de Lange E, Planchamp C, D'Alessandro M, Turlings TC, Ton J** (2009) Signal signature of aboveground-induced resistance upon belowground herbivory in maize. Plant J **59:** 292–302

**Frébortová J, Novák O, Frébort I, Jorda R** (2010) Degradation of cytokinins by maize cytokinin dehydrogenase is mediated by free radicals generated by enzymatic oxidation of natural benzoxazinones. Plant J **61:** 467–481

**Frey M, Chomet P, Glawischnig E, Stettner C, Grün S, Winklmair A, Eisenreich W, Bacher A, Meeley RB, Briggs SP, et al** (1997) Analysis of a chemical plant defense mechanism in grasses. Science **277:** 696–699

**Frey M, Schullehner K, Dick R, Fiesselmann A, Gierl A** (2009) Benzoxazinoid biosynthesis, a model for evolution of secondary metabolic pathways in plants. Phytochemistry **70:** 1645–1651

**Frey M, Spiteller D, Boland W, Gierl A** (2004) Transcriptional activation of *Igl*, the gene for indole formation in *Zea mays*: a structure-activity study with elicitor-active N-acyl glutamines from insects. Phytochemistry **65:** 1047–1055

**Frey M, Stettner C, Pare PW, Schmelz EA, Tumlinson JH, Gierl A** (2000) An herbivore elicitor activates the gene for indole emission in maize. Proc Natl Acad Sci USA **97:** 14801–14806

**Hamilton RH** (1964) A corn mutant deficient in 2,4-dihydroxy-7-methoxy-1,4-benzoxazin-3-one with an altered tolerance of atrazine. Weeds **12:** 27–30

**Iriti M, Faoro F** (2009) Chitosan as a MAMP, searching for a PRR. Plant Signal Behav **4:** 66–68

**Jonczyk R, Schmidt H, Osterrieder A, Fiesselmann A, Schullehner K, Haslbeck M, Sicker D, Hofmann D, Yalpani N, Simmons C, et al** (2008) Elucidation of the final reactions of DIMBOA-glucoside biosynthesis in maize: characterization of *Bx6* and *Bx7*. Plant Physiol **146:** 1053–1063

**Koch E, Slusarenko A** (1990) *Arabidopsis* is susceptible to infection by a downy mildew fungus. Plant Cell **2:** 437–445

**Leszczynski B, Dixon AFG** (1990) Resistance of cereals to aphids: interaction between hydroxamic acids and the aphid *Sitobion avenae* (Homoptera: Aphididae). Ann Appl Biol **117:** 21–30

**Livak KJ, Schmittgen TD** (2001) Analysis of relative gene expression data using real-time quantitative PCR and the 2(-Delta Delta C(T)) Method. Methods **25:** 402–408

**Luna E, Pastor V, Robert J, Flors V, Mauch-Mani B, Ton J** (2011) Callose deposition: a multifaceted plant defense response. Mol Plant Microbe Interact **24:** 183–193

**Macías FA, Molinillo JM, Varela RM, Galindo JC** (2007) Allelopathy—a natural alternative for weed control. Pest Manag Sci **63:** 327–348

**Maresh J, Zhang J, Lynn DG** (2006) The innate immunity of maize and the dynamic chemical strategies regulating two-component signal transduction in *Agrobacterium tumefaciens*. ACS Chem Biol **1:** 165–175

**Matthes MC, Bruce TJ, Ton J, Verrier PJ, Pickett JA, Napier JA** (2010) The transcriptome of cis-jasmone-induced resistance in *Arabidopsis thaliana* and its role in indirect defence. Planta **232:** 1163–1180

**Melanson D, Chilton MD, Masters-Moore D, Chilton WS** (1997) A deletion in an indole synthase gene is responsible for the DIMBOA-deficient phenotype of *bxbx* maize. Proc Natl Acad Sci USA **94:** 13345–13350

**Mena M, Ambrose BA, Meeley RB, Briggs SP, Yanofsky MF, Schmidt RJ** (1996) Diversification of C-function activity in maize flower development. Science **274:** 1537–1540

**Morant AV, Jørgensen K, Jørgensen C, Paquette SM, Sánchez-Pérez R, Møller BL, Bak S** (2008) beta-Glucosidases as detonators of plant chemical defense. Phytochemistry **69:** 1795–1813

**Niemeyer HM** (1988) Hydroxamic acids (4-hydroxy-1,4-benzoxazin-3-ones), defence chemicals in the gramineae. Phytochemistry **27:** 3349–3358

**Niemeyer HM** (2009) Hydroxamic acids derived from 2-hydroxy-2H-1,4-benzoxazin-3(4H)-one: key defense chemicals of cereals. J Agric Food Chem **57:** 1677–1696

**Niemeyer HM, Perez FJ** (1994) Potential of hydroxamic acids in the control of cereal pests, diseases, and weeds. *In* IKM Dakshini, FA Einhellig, eds, Allelopathy, Vol 582. American Chemical Society, Washington DC, pp 260–270

**Oikawa A, Ishihara A, Iwamura H** (2002) Induction of HDMBOA-Glc accumulation and DIMBOA-Glc 4-O-methyltransferase by jasmonic acid in poaceous plants. Phytochemistry **61:** 331–337

**Oikawa A, Ishihara A, Tanaka C, Mori N, Tsuda M, Iwamura H** (2004) Accumulation of HDMBOA-Glc is induced by biotic stresses prior to the release of MBOA in maize leaves. Phytochemistry **65:** 2995–3001

**Ramakers C, Ruijter JM, Deprez RH, Moorman AF** (2003) Assumption-free analysis of quantitative real-time polymerase chain reaction (PCR) data. Neurosci Lett **339:** 62–66

**Rashid MA, Gustafson KR, Cardellina JH II, Boyd MR** (1996) A benzoic acid glycoside from *Geniostoma antherotrichum*. Phytochemistry **41:** 1205–1207

**Rostás M** (2007) The effects of 2,4-dihydroxy-7-methoxy-1,4-benzoxazin-3-one on two species of *Spodoptera* and the growth of *Setosphaeria turcica* in vitro. J Pest Sci **80:** 35–41

**Rostás M, Ton J, Mauch-Mani B, Turlings TCJ** (2006) Fungal infection reduces herbivore-induced plant volatiles of maize but does not affect naïve parasitoids. J Chem Ecol **32:** 1897–1909

**Schlaeppi K, Abou-Mansour E, Buchala A, Mauch F** (2010) Disease resistance of Arabidopsis to *Phytophthora brassicae* is established by the sequential action of indole glucosinolates and camalexin. Plant J **62:** 840–851

**Schlaeppi K, Mauch F** (2010) Indolic secondary metabolites protect Arabidopsis from the oomycete pathogen *Phytophthora brassicae*. Plant Signal Behav **5:** 1099–1101

**Schmittgen TD, Livak KJ** (2008) Analyzing real-time PCR data by the comparative C(T) method. Nat Protoc **3:** 1101–1108

**Shkolnik-Inbar D, Bar-Zvi D** (2010) ABI4 mediates abscisic acid and cytokinin inhibition of lateral root formation by reducing polar auxin transport in *Arabidopsis*. Plant Cell **22:** 3560–3573

**Subbiah V, Reddy KJ** (2010) Interactions between ethylene, abscisic acid and cytokinin during germination and seedling establishment in Arabidopsis. J Biosci **35:** 451–458

**Ton J, D'Alessandro M, Jourdie V, Jakab G, Karlen D, Held M, Mauch-Mani B, Turlings TC** (2007) Priming by airborne signals boosts direct and indirect resistance in maize. Plant J **49:** 16–26

**Ton J, Flors V, Mauch-Mani B** (2009) The multifaceted role of ABA in disease resistance. Trends Plant Sci **14:** 310–317

**VanEtten HD, Mansfield JW, Bailey JA, Farmer EE** (1994) Two classes of plant antibiotics: phytoalexins versus "phytoanticipins". Plant Cell **6:** 1191–1192

**von Rad U, Hüttl R, Lottspeich F, Gierl A, Frey M** (2001) Two glucosyltransferases are involved in detoxification of benzoxazinoids in maize. Plant J **28:** 633–642

**Vysotskaya LB, Veselov SY, Kudoyarova GR** (2010) Effect on shoot water relations, and cytokinin and abscisic acid levels of inducing expression of a gene coding for isopentenyltransferase in roots of transgenic tobacco plants. J Exp Bot **61:** 3709–3717

**Yu Q, Tang C, Chen Z, Kuo J** (1999) Extraction of apoplastic sap from plant roots by centrifugation. New Phytol **143:** 299–304